Performance Analysis of Vacuum Insulation Panels Using Real Gas Equation for Mitigating Solar Heat Gain in Buildings

Divyanshu Sood, Pranaynil Saikia, Marmik Pancholi, and Dibakar Rakshit

1 Introduction

Vacuum insulation panels (VIPs) consist of dry core material embedded in a vacuum-tight cover called envelope (Liang et al. 2017), as shown in Fig. 1. The thermal conductivity of VIP varies with the core material. The suitable core materials for VIPs are fumed silica, polyurethane (PU) foam, glass fiber, and so on (Capozzoli et al. 2015). The fumed silica gives the best performance in terms of thermal conductivity when it is kept dry and evacuated. VIPs can provide 5–20 times lower thermal conductivity than that of conventional insulating materials (Brunner et al. 2014). Although the overall thermal conductivity of VIP depends considerably on the core material, it gets affected by the envelope material which is responsible for preventing the air and water permeation. In general, the nanostructure core material is desired for the core of VIP (Molleti et al. 2018; Liang et al. 2019). To maintain the desired thermal conductivity of the core, it is mandatory to maintain the vacuum inside the VIP. Getters and desiccants are used to maintain a suitable vacuum inside the VIP (Kalnæs and Jelle 2014).

The envelope maintains a vacuum inside the VIP by preventing the intake of water and air gases (Benson et al. 1994). Various envelope materials are used for this purpose. The envelope materials can either be metal film (MF) or metalized films (MFs) (Wegger et al. 2011). Metal films are laminated with a layer of polyethylene

D. Sood · P. Saikia · D. Rakshit (✉)
Centre for Energy Studies, Indian Institute of Technology Delhi, Hauz Khas, New Delhi 110016, India
e-mail: dibakar@iitd.ac.in

M. Pancholi
School of Engineering and Applied Sciences, Ahmedabad University, Ahmedabad, Gujrat 380009, India

H. Tyagi et al. (eds.), *New Research Directions in Solar Energy Technologies*,
Energy, Environment, and Sustainability,
https://doi.org/10.1007/978-981-16-0594-9_9

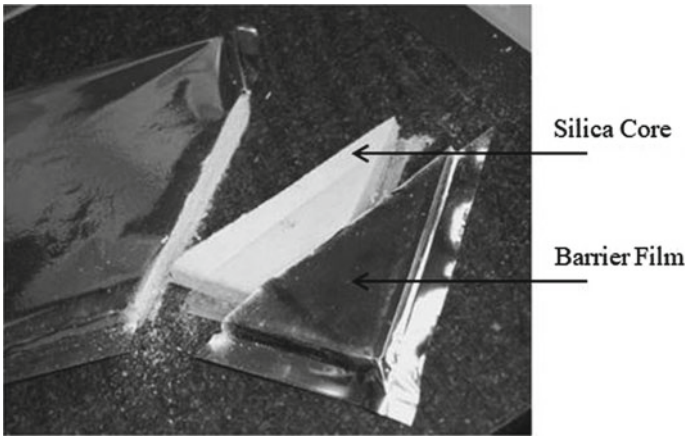

Fig. 1 Vacuum insulation panel (Simmler and Brunner 2005a)

terephthalate (PET) and metalized films have up to three layers of aluminum metalized polyethylene terephthalate (PET) or polypropylene (Tenpierik and Cauberg 2010). The envelope supports the vacuum for a longer period of time. The thermal conductivity of the core is a function of both air and water permeation. The pressure increase due to the intake of air and water across foil cover strongly depends on climatic conditions such as temperature, pressure, and relative humidity around VIP and also on the geometry of the panel (Alotaibi and Riffat 2014).

The total heat transfer through the VIP can take place via four different heat transfer processes: heat transfer via radiation, heat transfer via conduction in the core, heat transfer due to gas conduction, and heat transfer due to gas convection (Baetens et al. 2010). For convection to happen, bulk motion of molecules is required. In the present scenario, the concentration of molecules is very less inside the VIP, therefore the convection inside the VIP is not considered. So, the total heat flow is the summation of above-mentioned different heat transfer processes as given by Eq. (1),

$$Q_{\text{total}} = Q_r + Q_{cd} + Q_g \tag{1}$$

All these parameters should be minimum for insulation in buildings that results in an overall low thermal conductivity (Fricke et al. 2006). Lower the thermal conductivity of the insulation material, higher will be the thermal resistance which indicates less heat transfer. Thermal conductivity of core material depends on the amount of gas and water permeated into VIP. The permeation should be minimum and this can be achieved by selecting suitable envelope material with proper sealing (Kan et al. 2015). The increase in overall thermal conductivity of the VIP over time is called thermal conductivity aging. The thermal conductivity of the vacuum insulation panel depends upon gas permeation with time, water vapors formed inside the envelope, and water adsorbed on fumed silica core (Schwab et al. 2005a). To reduce the effect of parameters affecting the performance of VIP, getters and desiccants

are used. The getters remove the gas molecules from the evacuated space either by chemically combining with them or by adsorbing them whereas desiccants bind the water molecules (Xu et al. 2018). Batard et al. conducted a study on the thermal performance of VIP installed in buildings in winter and autumn season (cold climate) (Batard et al. 2018a). In the present study, the climate considered is hot and dry which is a major distinction from the previous work of Batard et al.

The ideal gas law considers gas molecule as point particle that does not occupy any space and is not attracted or repelled by other gas molecules, i.e., intermolecular interactions are nearly zero. The ideal gas equation is represented as Eq. (2),

$$P\nu = \frac{RT}{M} \tag{2}$$

To justify volume that a real gas molecule occupies, Van der Waals equation substitutes volume in ideal gas equation with $(V - b)$. The second modification in ideal gas law explains the molecular force of attraction. Van der Waals provided intermolecular attraction by adding a term a/V_m^2 to the observed pressure P in the equation. The constant 'a' provides a correction for the intermolecular forces and 'b' is a correction for finite molecular size. The Van der Waals equation can, therefore, be written as Eq. (3):

$$\left(P + \frac{n^2 a}{V^2}\right)(V - nb) = nRT \tag{3}$$

The present analysis emphasizes on using the Van der Waals equation for the performance analyses of VIP in terms of variation in internal pressure, thermal conductivity, service life. The previous studies used ideal gas equation for VIP analyses which does not provide a precise solution because, for air, to be considered as an ideal gas low pressure and high temperature is required. The key aspects of the present study were to investigate the performance of VIP considering air as a real gas to achieve more precise results and also to examine the effect of ambient temperature which is the function of solar radiation intensity falling on the surface.

2 Mathematical Model

The thermal performance of the VIPs is highly reliant on vacuum inside the envelope and gets disturbed by air and water permeation. The combined effect of air and water permeation inside the VIP increases the inside pressure and therefore thermal conductivity of core. This will further shorten the service life of a VIP. Under high temperature and low pressure, real gas behaves as an ideal gas. Here, the VIP is used for building application. The gas pressure is low inside the panel, which partially fulfills the ideal gas behavior requirements. However, the operating temperature of the VIP for the current application (20–50 °C) is much below the high-temperature

requirement for gas to behave ideally. Furthermore, with time the concentration of gas molecules increases inside the VIP with a subsequent increase in pressure. Under these circumstances, considering Van der Waals equation for the analysis of VIPs leads to a more realistic approach. In this mathematical model, both molecular volume and intermolecular force of attraction factors are included for calculating the increase in inside pressure due to air permeation which affects the thermal conductivity and service life significantly. Also, the study has been carried out for hot and dry climate (relative humidity < 55%) (Nayak and Prajapati 2006), so the effect of water on the degradation of the fumed silica core can be neglected and only solar radiation is considered for the analysis.

2.1 Determination of Air Permeation

The VIP envelope consists of different layers, so it is difficult to calculate the definite value of air permeation through it. There will always be some uncertainty in it. It can be expressed in terms of air transmission rate (ATR) and is given by Eq. (4). The air permeates through the surface of the laminate cover per panel area (ATR_A) from both the front and the rear side and also along the circumference of the panel (ATR_L). The increase in pressure inside VIP affects the service life of the panel. The pressure is increased due to the intake of air through the envelope (Yrieix and Pons 2018).

$$\mathrm{ATR}_{\mathrm{total}} = \left(A \times Q_{g,A} + L \times Q_{g,L}\right) \times \Delta P_{g,0} = \mathrm{ATR}_A.A + \mathrm{ATR}_L.L \tag{4}$$

Real gas equation considers the volume occupied by molecules of air and also the pressure change due to intermolecular forces of attraction. Using the real gas equation to solve for $P_{a(\mathrm{int})}$ as represented in Eq. (5).

$$P_{a(\mathrm{int})} = \frac{RTn}{V_{\mathrm{effective}} - nb} - \frac{an^2}{(V_{\mathrm{effective}})^2} \tag{5}$$

As a result of gas permeation, the pressure inside the core of the VIP increases and can be found out by following relation (Yrieix and Pons 2018; Simmler and Brunner 2005b).

$$\frac{\mathrm{d}p_{\mathrm{gas}}}{\mathrm{d}t} = \frac{Q_{\mathrm{gas,total}}\,\Delta p_{\mathrm{gas}}}{V_{\mathrm{effective}}}\left(\frac{T_m p_0}{T_0}\right)t = \frac{\mathrm{ATR}_{\mathrm{total}}}{V_{\mathrm{effective}}}\left(\frac{T_m p_0}{T_0}\right)t \tag{6}$$

where

$$V_{\mathrm{effective}} = V_{\mathrm{total}} \times \mathrm{Porosity} \tag{7}$$

Analytically solving Eq. (6) and assuming initial pressure inside the VIP to be zero, the final equation for the internal pressure change with time is given by Eq. (8),

$$p(t) = p_{\text{applied}} - \left(p_{\text{applied}} - p_{\text{initial}}\right) \times \mathrm{e}^{\frac{T_m \times p_0 \times Q_{\text{gas,total}}}{T_0 \times V_{\text{effective}}} \times t} \tag{8}$$

2.2 Determination of Thermal Conductivity

The high thermal performance of VIP is achieved when the core remains in the dry and evacuated state. The relation between the gas pressure and thermal conductivity is a result of the Knudsen number (Kan et al. 2015) and is formulated as Eq. (9). Knudsen number is a dimensionless number, given by Eq. (10), which is defined as the ratio of the mean free path in the gas phase to mean pore diameter. It plays a significant role in insulation materials where gases are under low pressure. Since the porosity of silica core is very high (>90%) and is under very low pressure, the air at ambient pressure will play an important role in degrading the quality of silica. However, considering the narrow pore size in porous silica, the free air conduction $\lambda_{g,0}$ is reduced due to the Knudsen effect. β is a constant which depends upon the nature of gas and temperature and its value is close to 1.5 (Hans et al. 2005).

$$\lambda_g = \frac{\lambda_{g,0}}{1 + 2 \times \beta \times Kn} \tag{9}$$

where *Kn* is the Knudsen number.

$$Kn = \frac{l_{\text{mean}}}{\delta} \tag{10}$$

$$l_{\text{mean}} = \frac{k_B T}{\sqrt{2\pi d_g^2 p_g}} \tag{11}$$

Each layer in the construction can be treated as thermal resistance and the thermal conductivity with time can be calculated using Eq. (12) (Nayak and Prajapati 2006). Equivalent thermal conductivity of VIP is then the sum of thermal conductivity in dry and evacuated state and thermal conductivity due to the air intake.

$$\lambda_{\text{core}}(t) = \lambda_{\text{evac}} + \lambda_g(t) \tag{12}$$

Also, due to the thermal bridge effect at edges, the thermal conductivity of VIP changes. In this study, the thermal bridge effect at edges is only considered as the surface area of VIP is large. So, adding a thermal bridge effect into Eq. (12), the equivalent thermal conductivity of VIP can be represented by Eq. (13). The thermal

Table 1 Input parameters

Properties	Barrier envelope materials			Source
	AF	MF-2	MF-3	
ATR_A ($cm^3\ m^{-2}\ day^{-1}$)	–	–	0.0080	Hans et al. (2005)
ATR_L ($cm^3\ m^{-1}\ day^{-1}$)	0.0018	0.0039	0.0091	Hans et al. (2005)
Activation energy (E_a) (kJ mol^{-1})	26	28	35	Schwab et al. (2005d)
$\psi(d)$ (W $m^{-1}\ K^{-1}$)	0.07	0.01	0.01	Nayak and Prajapati (2006)
Dry core density (kg m^{-3})	200			Quenard and Sallee (2005)
Specific heat (J $kg^{-1}\ K^{-1}$)	800			Herek and Nsofor (2014)
$\lambda_{g,0}$ (W $m^{-1}\ K^{-1}$)	25.7×10^{-3}			Schwab et al. (2005b)
$P_{1/2,g}$ (Pa)	593			Schwab et al. (2005c)
Van der Waals constant 'a'	134,762.25 × 10-6 Pa m^6 mol^{-2}			Handout (n.d.)
Van der Waals constant 'b'	36.6 × 10-6 m^3 mol^{-1}			Handout (n.d.)

bridge at edge depends upon linear thermal transmittance, the thickness of the edge, the total length of an edge, and total area of the edges (Nayak and Prajapati 2006).

$$\lambda_{\text{eq}}(t) = \lambda_{\text{evac}} + \lambda_g(t) + \psi(d) \times \frac{d \times l}{A} \tag{13}$$

It is assumed that the pressure increase inside the VIP is caused by dry air infusion (Schwab et al. 2005c). Consider the thermal conductivity of the center of the panel in the evacuated and dry state equal to 4×10^{-3} W m^{-1} K^{-1} (Batard et al. 2018b). Further the above-mentioned factors in Eq. (13) can be calculated using Eq. (14) (Tenpierik and Van Der Spoel 2007):

$$\lambda_g(t) = \frac{\lambda_{g,0}}{1 + \frac{p_{1/2,g}}{p_g(t)}} \tag{14}$$

where $p_g = p_{g,e}\left(1 - e^{\frac{-t}{\tau_g}}\right)$. τ_g is the time constant for air and can be estimated by:

$$\tau_g = \frac{\varepsilon V}{\text{ATR}(T, \emptyset)} \times \frac{T_0}{p_0 T} \tag{15}$$

According to the Arrhenius equation, the ambient temperature greatly affects the air permeance. The equation explains the logarithmic relation between the temperature and activation energy, represented by Eq. (16).

$$Q(T) = Q(T_0) e^{\frac{E_a}{R}\left(\frac{1}{T_0} - \frac{1}{T}\right)} \tag{16}$$

For solving various equations as discussed, input parameters are shown in Table 1. The values of ATR are at 23 °C, 50% RH, and 1 bar atmospheric pressure for different envelope materials. The size of the panel is 100 × 100 × 2 cm^3.

3 Heat Transfer Analysis

The transient one-dimensional conduction heat transfer in a concrete wall having VIP has been carried out in which temperature is a function of x (wall thickness) and t (time). The total thickness of the wall was chosen to be 260 mm including the thickness of VIP as 20 and 240 mm as the thickness of the concrete wall (Saikia et al. 2018a, b). The domain is divided into N elements of Δx each as shown in Fig. 2. The aim of study is to show the variation in heat gain inside the room when VIP analysis is done considering air as a real gas.

In central difference approximation of the second derivative with respect to x, the nodal equation will involve T_{i-1}, T_i and T_{i+1}. In explicit form, the second derivative with respect to x is evaluated with all the known temperatures at time t. In its nodal form, the equation may be written as Eq. (17) (Venkateshan 2009). The analysis was carried out for 21,600 s with a time step of 1 s. The smaller time step was chosen for better precision.

$$T_{i,j+1} = F_o\left[T_{i-1,j} + T_{i+1,j}\right] + [1 - 2\text{Fo}]T_{i,j} \tag{17}$$

where Fo is Fourier number and is formulated as $\text{Fo} = \frac{\alpha \Delta t}{\Delta x^2}$, $t = (j-1)\Delta t$ at $t = 0$, $j = 1$.

The two ends of the wall are open to the environment and convectively transfer heat to the surroundings at a temperature T_∞ via heat transfer coefficient h. The nodal equation representing the temperature at the wall ends is as follows

$$T_{1,j+1} = T_{1,j}[1 - 2\text{Fo}(1 + \text{Bi})] + 2F_o \times \text{Bi} \times T_\infty + 2F_o T_{2,j} \tag{18}$$

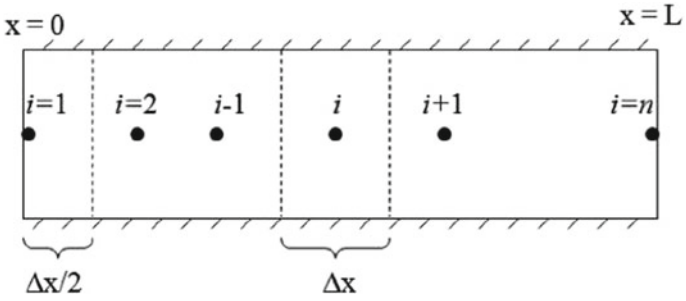

Fig. 2 1-D transient heat transfer along the wall

where Bi is the elemental Biot number and is given by $\mathrm{Bi} = \frac{h\Delta x}{k}$.

Sol–air temperature is computed by Eq. (19) to combine the effects of solar radiation and ambient temperature for heat transfer analysis (Sharma and Rakshit 2017; Krarti and Ihm 2009). The analysis is done for the Jodhpur city of Rajasthan (Nayak and Prajapati 2006). The sol–air temperature was calculated considering solar radiation for 6 h (11 AM to 5 PM) for the month of May. The average ambient temperature was around 312.55 K, and the corresponding sol–air temperature was calculated to be 329.6 K. The initial temperature was 303 K at the very first node. Either solar irradiance or temperature on the south wall is maximum for this period of time.

$$T_{\mathrm{sol}} = T_0 + \frac{\alpha_s \times I}{h} \tag{19}$$

The thermal performance of the VIP in a concrete embedded VIP wall is evaluated using transient heat transfer analysis. The deviation in thermal performance of VIP is evaluated in terms of reduced heat gain and variation in inside and outside temperature which changes due to the location of the VIP into the concrete wall. The optimum location of VIP is investigated by positioning the VIP at three different locations, i.e., the inner side of the wall, center of the wall, and on the outer side of the concrete VIP wall assembly as shown in Fig. 3. Heat ingress through a wall carrying VIP with different thermal conductivities obtained by considering air as an ideal gas and a real gas is compared for the given geographical conditions.

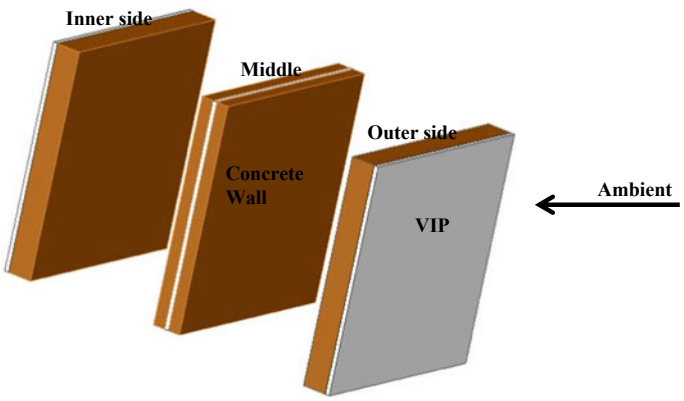

Fig. 3 Different location of VIP in the concrete wall

4 Ideal Gas Analogy

If volume occupied by air molecules and intermolecular forces of attraction, i.e., '*a*' and '*b*' is assumed to be negligible, then the air acts as an ideal gas. In the present model, by equating Van der Waals constants, i.e., a and b to zero in Eq. (5) and calculating further, a similar trend in results with relative error in the permissible range were attained as that using the ideal gas equation. Moreover, further calculations authenticate the present model more accurately as the thermal conductivity and internal pressure lies in the allowable deviation range as calculated using ideal gas, as illustrated by Figs. 4 and 5, respectively.

Also, the grid independence study was performed to optimize the number of nodes to carry the heat transfer analysis for VIP-concrete composite wall.

The numerical model developed for transient heat transfer study was tested for grid independence in order to institute the reliability of the model demonstrated in Fig. 6. For this, the number of nodes in the VIP wall is varied keeping the wall thickness the same. The VIP is placed on the inside of the wall and south wall irradiance is taken. The number of nodes in the VIP wall is varied from 26 to 234 nodes with an increment of 26 nodes in every step. Further, calculations are performed with 182 nodes after which the graph becomes asymptotic with dQ value of 4.31 kJ.

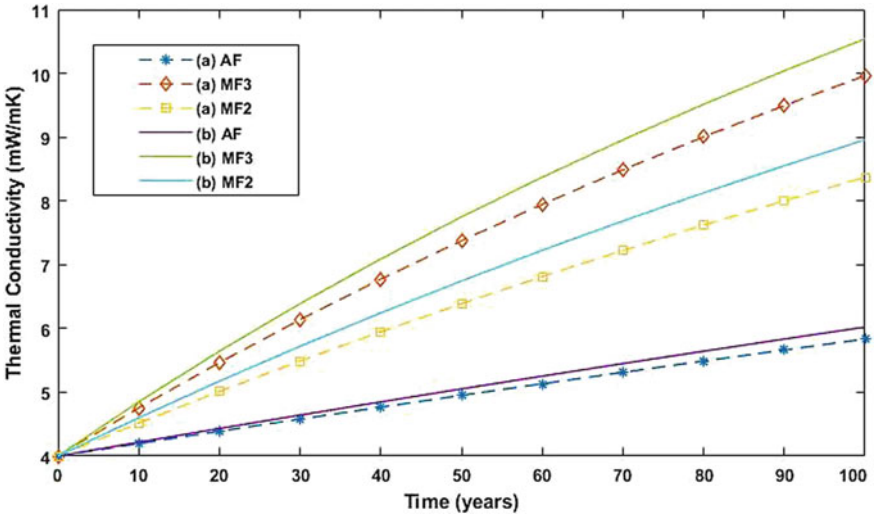

Fig. 4 **a** Thermal conductivity variation with time as per (Simmler and Brunner 2005a) (dotted lines) and **b** as per the present study (continuous lines)

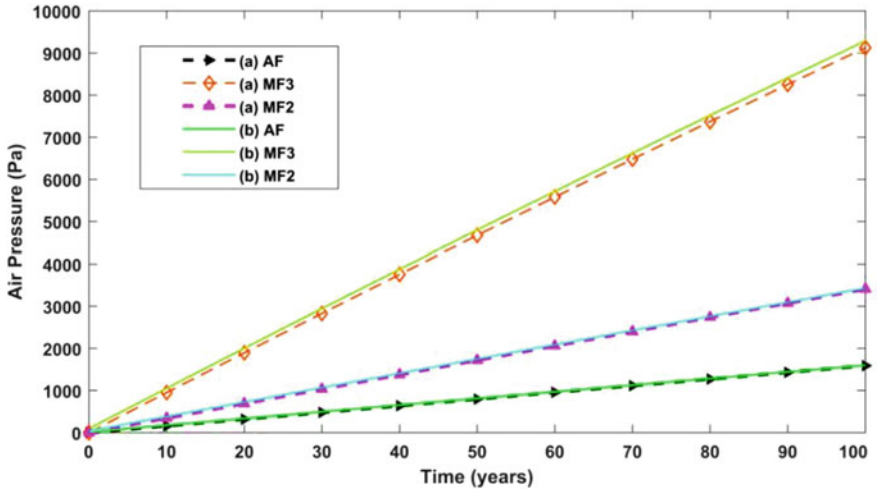

Fig. 5 **a** Variation in inside air pressure with time as (Simmler and Brunner 2005a) (dotted lines) and **b** as per the present study (continuous lines)

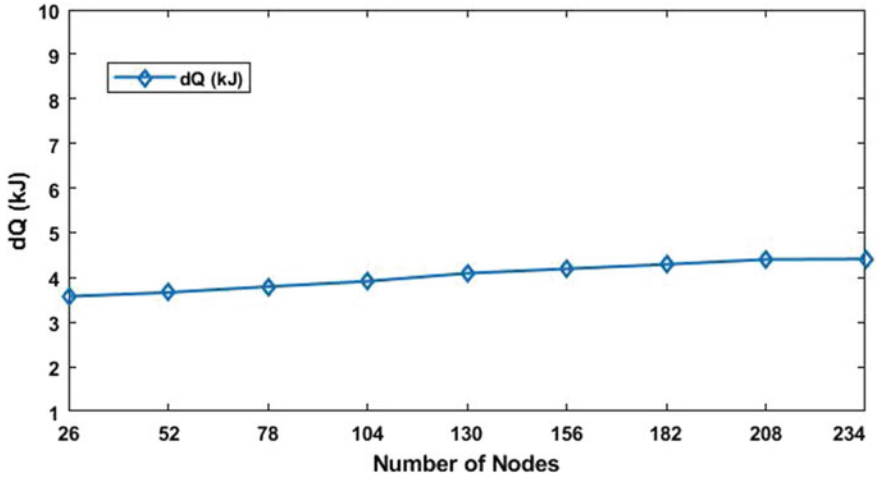

Fig. 6 Grid independence study

5 Results and Discussion

5.1 Comparison Analysis

The values of ATR for envelope material are used and calculations are performed using equations discussed previously. The ATR values are at 23 °C and 50% RH. By

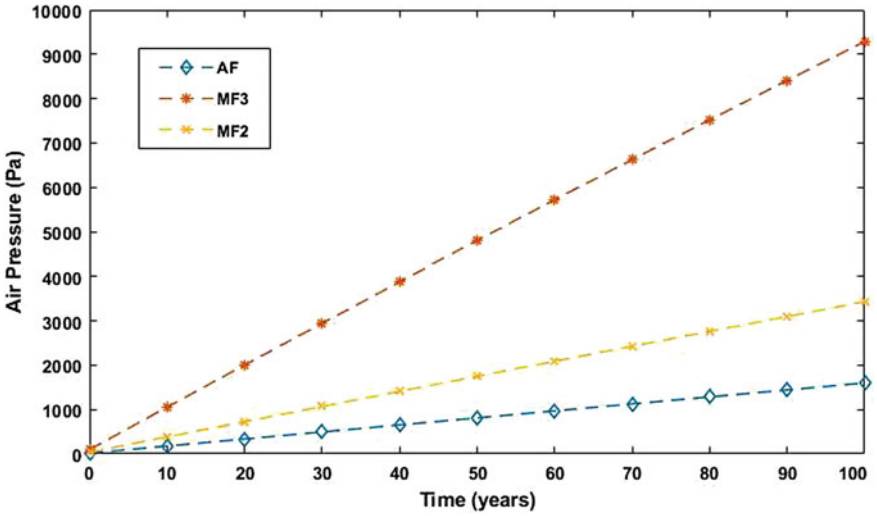

Fig. 7 Variation in inside air pressure with time for different envelope material

using Eq. (8), the air pressure with respect to time is calculated. Values are recorded assuming constant climatic conditions during the entire period. Similar variations in the parameters are observed when Van der Waals constants are considered. The study conducted by Wegger et al. (2011) neglected the thermal bridge effect (Wegger et al. 2011). To compare the present findings with the results of Wegger et al. (2011), the thermal bridge effect is neglected in Sect. 5.1.

Figure 7 depicts the variation in air pressure inside the VIP with time. Equation (8) is used to determine the variation of inside air pressure with time. The pressure increase is due to the air permeation inside the VIP through the envelope pores and sealing. It is because of the reason that different envelope materials have different resistance to air permeation because of the presence of multiple layers. The results got deviated from the prevailing results of the ideal gas equation when calculations were carried out using Van der Waals equation. Since Van der Waals equation considers the volume occupied by the air molecules that degrade the core of the VIP. Hence, the thermal conductivity increases.

The result comparison for the ideal gas equation and Van der Waals equation is mentioned in Table 2 consisting of different envelope materials. The curve for AF embedded VIP shows that internal air pressure is 1.62% more when analyzed using Van der Waals equation as compared to ideal gas for 50 years. With the increase in load on panel, i.e., atmospheric pressure, the rate of air ingression increases. Air permeation also depends upon the type of envelope, the thickness of envelope material, and geometrical specifications of the VIP. For a relatively shorter period of time (less than 30 years), the difference in pressure values calculated using the two different equations is not marginal. For buildings located in regions susceptible to frequent natural calamities (earthquake, tornado, etc.), the overall service life of the

Table 2 Variation in inside pressure (in Pa) due to air permeation

Envelope material		15 years	30 years	45 years	50 years
AF	Ideal	240.08	479.6	718.544	798.1
	Real	255.86	494.2	731.8935	811
	% increase (%)	6.5	3.04	1.8	1.62
MF-2	Ideal	519.4	1036.1	1550.1	1720.9
	Real	553.8	1068	1579.6	1749.5
	% increase (%)	6.62	3.08	1.9	1.66
MF-3	Ideal	1424.8	2829.6	4214.6	4671.9
	Real	1530.1	2945.5	4340.9	4801.6
	% increase (%)	7.39	4.10	2.99	2.78

building will be shorter and within this period the pressure calculation with the real gas equation is justified as illustrated by the difference in Table 2.

Equation (13) is used to calculate the thermal conductivity of VIP and results are shown in Fig. 8. The trend shows the direct relation between the time and thermal conductivity of the VIP. Internal pressure is a function of air ingression through envelope which further affects the thermal conductivity. The fumed silica core adsorbs the air molecules on its surface that are responsible for core degradation and consequently the performance of the VIP. The thermal conductivity values are highest for MF-3 envelope embedded VIP followed by MF-2 and are lowest for AF. Moreover, Table 3 compares the thermal conductivity result calculated by using the ideal gas

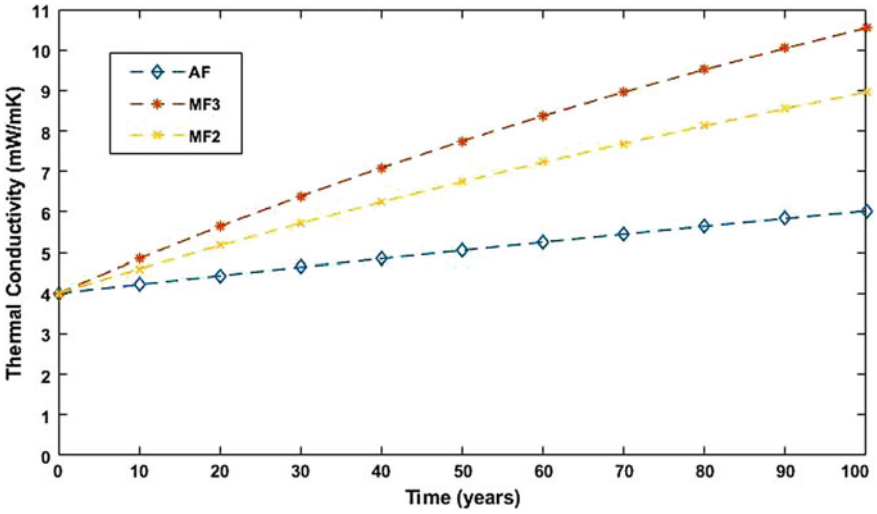

Fig. 8 Thermal conductivity variations with time for different envelope materials

Table 3 Variation in thermal conductivity (mW m^{-1} K^{-1})

Envelope material		15 years	30 years	45 years	50 years
AF	Ideal	4.2930	4.5794	4.8594	4.9514
	Real	4.3252	4.6422	4.9514	5.0527
	% increase	0.75	1.37	1.89	2.05
MF-2	Ideal	4.7668	5.489	6.1705	6.3891
	Real	4.8901	5.7205	6.4970	6.7447
	% increase	2.58	4.22	5.29	5.57
MF-3	Ideal	5.1152	6.1373	7.0776	7.3745
	Real	5.2530	6.3891	7.4241	7.7489
	% increase	2.69	4.10	4.89	5.08

Table 4 Service life of VIP

Envelope material	Service life (years)		% decrease in service life
	Ideal gas equation	Real gas equation	
AF	250	220	12
MF-2	92	77	16.3
MF-3	65	53	18.46

equation and the Van der Waals equation. It has been found that the variation is between 2 and 6% for the service life of 50 years.

Table 4 compares the results for the service life of VIP for different envelope materials. The increase of thermal conductivity over time reduces the service life of the VIP. Service life is defined as the time elapsed from the moment of manufacturing until the moment thermal conductivity exceeds limiting value as prescribed. Service life depends on the permeation inside VIP and external environmental conditions. Limiting value is set at 8×10^{-3} W m^{-1} K^{-1} (Schwab et al. 2005c). The results vary appreciably when calculated using the real gas equation. The maximum variation is observed in VIP with MF-3 envelope material, i.e., 18.46%. Using VIP with AF envelope material gives the highest service life, i.e., 220 years. Environmental conditions such as relative humidity, temperature, and solar irradiance affect the aging of the VIP. Getters and desiccants are provided inside the VIP which adsorb the air molecules so that the core remains in the dry and evacuated state for a longer period of time. This measure reduces thermal conductivity aging and increases service life.

The area of the wall is 4×3 m^2 (Ramos 1990). To evaluate the heat gain inside the room through the wall, the VIP was placed at three locations, viz. inner, center, and outer side. When the VIP was placed on the innermost side of the wall, the VIP concrete wall combination results in minimum heat gain inside the room through the wall and values are presented in Table 5. It is because of the reason that VIP is not directly exposed to solar radiation which reduces the direct environmental impact on it and also improves its thermal performance.

Table 5 Heat gain at different locations of VIP

Location of VIP	Heat gain (kJ)		
	AF	MF-2	MF-3
Inside	115.9091	93.2487	93.2487
Center	13,750.912	13,750.912	13,750.912
Outside	6472.786	14,388.838	14,546.298

Table 6 Heat gain comparison for MF-2 embedded VIP

Envelope material	Time (years)	Thermal conductivity (mW m^{-1} K^{-1})		dT (K)		Heat transfer, Q (kJ)		dQ (real-ideal) (kJ)
		Ideal	Real	Ideal	Real	Ideal	Real	
MF-2	10	4.516	4.600	0.039	0.039	89.153	89.647	0.494
	20	5.012	5.173	0.041	0.042	93.405	94.893	1.487
	30	5.489	5.720	0.043	0.044	97.951	100.427	2.475
	40	5.947	6.243	0.045	0.047	102.92	106.357	3.430
	50	6.389	6.744	0.048	0.049	108.15	112.475	4.317
	60	6.814	7.224	0.050	0.052	113.36	118.540	5.174
	70	7.224	7.684	0.052	0.055	118.54	124.630	6.089
	80	7.620	8.123	0.054	0.057	123.76	130.610	6.847
	90	8.002	8.550	0.057	0.060	128.89	136.520	7.626
	100	8.370	8.953	0.059	0.063	133.99	142.145	8.155

The heat gains through VIP–concrete composite wall when calculated using two different equations for MF-2 embedded VIP placed on the inner side of the wall are shown in Table 6. There was an 8.15 kJ of additional heat gain inside the room when the VIP–concrete composite wall was analyzed considering air as a real gas. Aforementioned thermal conductivity calculated using Van der Waals equation is 5–6% more when analyzed considering air as an ideal gas. Thermal conductivity directly affects the heat transfer rate as it permits more heat to pass through the wall.

5.2 Heat Transfer Analysis Considering Thermal Bridge

To calculate the heat gain inside the room through the concrete–VIP composite wall, the equivalent thermal conductivity of the VIP is calculated using Eq. (13), which also accounts for the thermal bridge effect. The thermal bridge has a significant effect on the thermal conductivity of AF embedded VIP as compared to other two envelope materials, i.e., MF-2 and MF-3 as shown in Tables 7, 8 and 9. Thermal bridging has an adverse effect on the overall performance of the VIP. The AF laminate reduces

Table 7 Heat transfer for AF embedded VIP

Time (years)	Thermal conductivity (mW m^{-1} K^{-1})	dT (K)			Heat transfer (kJ)
		T_{wall} (K)	T_i (K)	dT	
20	7.2317	297.0526	297	0.0526	118.666
40	7.6492	297.0551	297	0.0551	124.147
60	8.0530	297.0575	297	0.0575	129.633
80	8.4438	297.0599	297	0.0599	135.015
100	8.8224	297.0622	297	0.0622	140.286

Table 8 Heat transfer for MF-2 embedded VIP

Time (years)	Thermal conductivity (mW m^{-1} K^{-1})	dT (K)			Heat transfer (kJ)
		T_{wall} (K)	T_i (K)	dT	
20	5.5733	297.0439	297	0.0439	98.9727
40	6.6438	297.0493	297	0.0493	111.2145
60	7.6245	297.0549	297	0.0549	123.8394
80	8.5273	297.0604	297	0.0604	136.1448
100	9.3583	297.0656	297	0.0656	147.9302

Table 9 Heat transfer for MF-3 embedded VIP

Time (years)	Thermal conductivity (mW m^{-1} K^{-1})	dT (K)			Heat transfer (kJ)
		T_{wall} (K)	T_i (K)	dT	
20	6.0438	297.0461	297	0.0461	104.0097
40	7.4895	297.0541	297	0.0541	122.0332
60	8.7708	297.0619	297	0.0619	139.5855
80	9.9142	297.0692	297	0.0692	155.9366
100	10.9408	297.0758	297	0.0758	170.9716

the air permeation significantly and thereby increasing the service life of the VIP. However, because of the high thermal conductivity of aluminum (210 W m^{-1} K^{-1}) as compared to core thermal conductivity (0.004 W m^{-1} K^{-1}), the contribution of thermal bridging is higher. In contrast, the MF laminates show more increase in thermal conductivity but are less affected by thermal bridging due to polymer layers. Therefore, the combined effect of air permeation and thermal bridging could suggest that MF laminates are more suitable for building applications for the service life of 40–50 years.

6 Conclusions

1. A comprehensive study of VIP's aging characteristics has been conducted. The study illustrates the mathematical modeling of thermal performance of VIP considering air as real gas. The results vary when solved using Van der Waals equation instead of the ideal gas equation. The results for pressure increase inside the VIP and thermal conductivity deviate by 3–7% and 2–5% for MF-3 embedded VIP, respectively.
2. The service life of VIP is affected by 12% in AF embedded VIP and maximum decrease is observed for MF-3 embedded VIP, i.e., 18%. Therefore, using AF embedded VIP is the best option for longer service life as inferred from the findings of the present study.
3. It is observed that when VIP is placed on the inner side of the wall, it results in minimum heat gain inside the room through the wall as compared to other two locations, i.e., at the outer surface and at the center. When placed in the center of the wall the heat gain is the same as that with no VIP installed on the wall.
4. There is approximately 2.8 mW m^{-1} K^{-1} increase in thermal conductivity for AF embedded VIP when the thermal bridge at edges is also considered for heat transfer analysis. The thermal bridge effect is less significant for MF-2 and MF-3 envelope material.
5. It is clearly visible from the analysis that the thermal bridge has a significant effect on the performance of the VIP. It increases the equivalent thermal conductivity of VIP which leads to more heat gain and decrease in the service life.
6. The results show appreciable variation in performance of VIP for up to 50 years, which is the average life of the building. This justifies the consideration of air as a real gas for a more realistic approach.

References

Alotaibi SS, Riffat S (2014) Vacuum insulated panels for sustainable buildings: a review of research and applications. Int J Energy Res. https://doi.org/10.1002/er.3101

Baetens R, Jelle BP, Thue JV, Tenpierik MJ, Grynning S, Uvsløkk S, Gustavsen A (2010) Vacuum insulation panels for building applications: a review and beyond. Energy Build 42:147–172. https://doi.org/10.1016/j.enbuild.2009.09.005

Batard A, Duforestel T, Flandin L, Yrieix B (2018a) Prediction method of the long-term thermal performance of Vacuum Insulation Panels installed in building thermal insulation applications. Energy Build 178:1–10. https://doi.org/10.1016/j.enbuild.2018.08.006

Batard A, Duforestel T, Flandin L, Yrieix B (2018b) Modelling of long-term hygro-thermal behaviour of vacuum insulation panels. Energy Build 173:252–267. https://doi.org/10.1016/j.enbuild.2018.04.041

Benson DK, Potter TF, Tracy CE (1994) Design of a variable-conductance vacuum insulation

Brunner S, Simmler H, Brunner S (2014) Thermal properties and service life of vacuum insulation panels (VIP) Service Life Prediction of VIPs-Project on comparing reality with former predictions

View project Thermal properties and service life of vacuum insulation panels (VIP), https://www.researchgate.net/publication/228681787
Capozzoli A, Fantucci S, Favoino F, Perino M (2015) Vacuum insulation panels: analysis of the thermal performance of both single panel and multilayer boards. Energies. https://doi.org/10.3390/en8042528
Fricke J, Schwab H, Heinemann U (2006) Vacuum insulation panels—exciting thermal properties and most challenging applications. Int J Thermophys. https://doi.org/10.1007/s10765-006-0106-6
Handout (n.d.) che31.weebly.com/uploads/3/7/4/3/3743741/handout_e-realgasconstants.pdf. Accessed 19 June 2019
Hans S, Samuel B, Ulrich H, Schwab H, Kumar K, Phalguni M, Daniel Q, Hébert S, Klaus N, Cornelia S, Esra K, Martin T, Hans C, Markus E (2005) Vacuum insulation panels—study on VIP-components and panels for service life prediction of VIP in building applications (Subtask A), HiPTI—High Perform. Therm. Insul.—IEA/ECBCS Annex 39
Herek SJ, Nsofor EC (2014) Performance of vacuum insulation panels in building energy conservation, pp 149–160
Kalnæs SE, Jelle BP (2014) Vacuum insulation panel products: a state-of-the-art review and future research pathways. Appl Energy. https://doi.org/10.1016/j.apenergy.2013.11.032
Kan A, Kang L, Wang C, Cao D (2015) A simple and effective model for prediction of effective thermal conductivity of vacuum insulation panels. Futur Cities Environ. https://doi.org/10.1186/s40984-015-0001-z
Krarti M, Ihm P (2009) Implementation of a building foundation heat transfer model in EnergyPlus. J Build Perform Simul 2:127–142. https://doi.org/10.1080/19401490802613610
Liang Y, Wu H, Huang G, Yang J, Wang H (2017) Thermal performance and service life of vacuum insulation panels with aerogel composite cores. Energy Build 154:606–617. https://doi.org/10.1016/j.enbuild.2017.08.085
Liang Y, Ding Y, Liu Y, Yang J, Zhang H (2019) Modeling microstructure effect on thermal conductivity of aerogel-based vacuum insulation panels. Heat Transf Eng 1–14. https://doi.org/10.1080/01457632.2019.1576443
Molleti S, Lefebvre D, van Reenen D (2018) Long-term in-situ assessment of vacuum insulation panels for integration into roofing systems: Five years of field-performance. Energy Build 168:97–105. https://doi.org/10.1016/j.enbuild.2018.03.010
Nayak JK, Prajapati JA (2006) Handbook on energy conscious buildings. In: Handb. Energy Conscious Build., Solar Energy Centre, Ministry of Non-conventional Energy sources, Government of India, New Delhi, India
Quenard D, Sallee H (2005) Micro-nano porous materials for high performance thermal insulation micro-nano porous materials for high performance. In: 2nd international symposium on nanotechnology in construction, pp 1–10
Ramos JI (1990) Basic heat transfer. Appl Math Model 14:666. https://doi.org/10.1016/0307-904X(90)90027-3
Saikia P, Azad AS, Rakshit D (2018a) Thermodynamic analysis of directionally influenced phase change material embedded building walls. Int J Therm Sci 126:105–117. https://doi.org/10.1016/j.ijthermalsci.2017.12.029
Saikia P, Azad AS, Rakshit D (2018b) Thermal performance evaluation of building roofs embedded PCM for multi-climatic zones. Springer, Singapore, pp 401–423. https://doi.org/10.1007/978-981-10-7188-1_18
Schwab H, Heinemann U, Beck A, Ebert H-P, Fricke J (2005a) Dependence of thermal conductivity on water content in vacuum insulation panels with fumed silica kernels. J Therm Envel Build Sci 28:319–326. https://doi.org/10.1177/1097196305051792
Schwab H, Heinemann U, Wachtel J, Ebert HP, Fricke J (2005b) Predictions for the increase in pressure and water content of Vacuum Insulation Panels (VIPs) integrated into building constructions using model calculations. J Therm Envel Build Sci 28:327–344. https://doi.org/10.1177/1097196305051793

Schwab H, Heinemann U, Beck A, Ebert HP, Fricke J (2005c) Prediction of service life for vacuum insulation panels with fumed silica kernel and foil cover. J Therm Envel Build Sci. https://doi.org/10.1177/1097196305051894

Schwab H, Heinemann U, Beck A, Ebert HP, Fricke J (2005d) Permeation of different gases through foils used as envelopes for vacuum insulation panels. J Therm Envel Build Sci. https://doi.org/10.1177/1097196305051791

Sharma P, Rakshit D (2017) Quantitative assessment of orientation impact on heat gain profile of naturally cooled buildings in India. Adv Build Energy Res 11:208–226. https://doi.org/10.1080/17512549.2016.1215261

Simmler H, Brunner S (2005a) Vacuum insulation panels for building application: basic properties, aging mechanisms and service life. Energy Build. https://doi.org/10.1016/j.enbuild.2005.06.015

Simmler H, Brunner S (2005b) Vacuum insulation panels for building application: Basic properties, aging mechanisms and service life. Energy Build 37:1122–1131. https://doi.org/10.1016/j.enbuild.2005.06.015

Tenpierik MJ, Cauberg JJM (2010) Encapsulated vacuum insulation panels: theoretical thermal optimization. Build Res Inf 38:660–669. https://doi.org/10.1080/09613218.2010.487347

Tenpierik M, Van Der Spoel W (2007) Simplified analytical models for service life prediction of a vacuum insulation panel Double Face 2.0 View project Research through Design for Values View project Analytical VIP Service Life Prediction Model Simplified Analytical Models for Service Life Prediction of a Vacuum Insulation Panel, https://www.researchgate.net/publication/284778729

Venkateshan SP (2009) Heat transfer. Ane Books

Wegger E, Jelle BP, Sveipe E, Grynning S, Gustavsen A, Baetens R, Thue JV (2011) Aging effects on thermal properties and service life of vacuum insulation panels. J Build Phys 35:128–167. https://doi.org/10.1177/1744259111398635

Xu T, Chen Z, Yang Y, Chen Z, Zhang J, Wu C, Liu Y (2018) Correlation between the thermophysical properties and core material structure of vacuum insulation panel: role of fiber types. Fibers Polym 19:1032–1038. https://doi.org/10.1007/s12221-018-7949-x

Yrieix B, Pons E (2018) New method to assess the air permeance into vacuum insulation panel. Vacuum. https://doi.org/10.1016/j.vacuum.2017.11.033